

6. Optimal Candle Solution

University of Surrey, Guildford GU2 7XH, United Kingdom

1 Introduction

This manuscript presents our solution to Problem 6, the Optimal Candle Problem, from the International Physicists' Tournament (IPT) 2025. The problem is defined as follows: Maximize the luminosity of a candle by varying its size and shape for a chosen wick. What shape should it have to ensure that, when the wick has fully burnt out, all the wax has also completely vaporized away? To address this, we developed theoretical models to identify the ideal candle geometry that ensures constant luminosity and complete wax vaporization. A subsequent model determined the optimal size for this geometry. These models were experimentally validated using beeswax candles, where illuminance was measured with a lux meter, and mass loss percentages were compared for different shapes and sizes with a chosen wick. Our findings provide insights into designing candles that maximize luminosity, ensure efficient wax usage, and leave no residual wax, contributing to improved understanding and practical applications in candle performance.

2 Theoretical Model

The geometry of the wick is a critical determinant of candle performance, directly influencing wax absorption, combustion stability, and the longevity of the flame.^[1] The wick is a capillary system that draws molten wax upward into the flame, where it vaporises and combusts.^{[1][2]} This process is governed by the radius and porosity of the wick, which define the maximum rate of wax absorption. Any mismatch between the wick's capacity and molten wax's availability can lead to inefficient burning and flame instability.

Maintaining a consistent balance between wax melting and evaporation becomes challenging for candles with non-uniform shapes, such as cones.^[2] A conical candle has a larger volume of wax at the top/bottom, requiring a thicker/thinner wick to ensure sufficient wax absorption and combustion. However, as the candle burns and its radius decreases, a wick of constant thickness may absorb too much or too little wax than is available or it may not draw enough wax. This imbalance can cause incomplete combustion, leading to the formation of soot and carbon build-up, which affects the function of the candle.^[1]

Uniform geometries, such as cylindrical candles, are preferred because they facilitate radial heat distribution around the flame.^[2] This symmetrical shape ensures that heat is evenly dispersed in all directions from the flame, promoting consistent melting of wax surrounding the wick. Therefore, it can be deduced cylindrical candles maintain a stable burning rate and efficiently feed the flame with melted wax, extending their useful life and maximising fuel efficiency. The uniform geometry inherently supports the even thermal balance required for optimal candle performance.

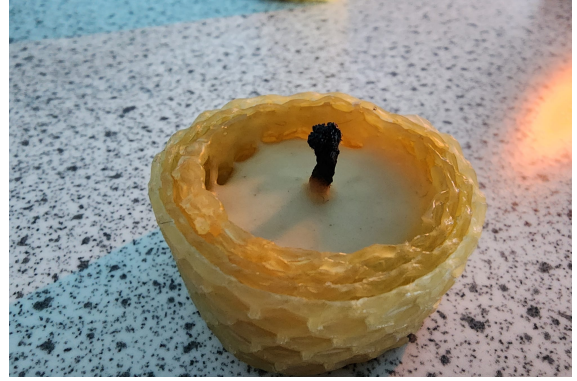


Figure 1: Example of candle tunnelling observed in a cylindrical candle (Candle No. 1).

In contrast, non-uniform shapes, such as cuboidal candles, disrupt this balance because they cannot achieve radial heat distribution due to their 2-dimensional projection on the cross-sectional area not being a circle. The asymmetry of these designs creates uneven thermal gradients, with insufficient heat reaching areas such as the corners. Consequently, the wax in these regions often remains unmelted, leading to tunnelling.

Candle tunnelling occurs when the heat from the flame is insufficient to melt the wax near the edges of the candle. As shown in Figure 1, the wax close to the wick is depleted, forming a tunnel-like depression, while the surrounding wax remains intact. This phenomenon is particularly common in candles with poor radial heat distribution or wicks of improper size. This phenomenon occurs when wax near the wick is consumed while wax at the edges remains intact, reducing the fuel efficiency and lifespan of the candle. The lack of consistent radial heat distribution in non-uniform geometries makes them less effective and practical compared to cylindrical designs.^[3]

Cylindrical candles also benefit from the self-regulating nature of the candle system. The flame height and temperature adjust in response to the wax supply: when the wick draws more wax than necessary, the flame grows larger, increasing heat and accelerating wax melting. Conversely, when the wax supply diminishes, the flame shrinks, reducing heat and conserving wax.^[4] This feedback mechanism allows the cylindrical candle to maintain a steady flame throughout its burn time. In contrast, irregularly shaped candles may disrupt this balance as a result of uneven wax melting, leading to over- or under-feeding of the flame and compromising the self-regulating process.

Ultimately, the compatibility between the wick and candle body geometry is essential to optimise performance. Cylindrical candles with cylindrical wicks achieve a harmonious balance of heat distribution, wax supply, and combustion dynamics, ensuring clean, stable, and efficient burn.^[1] Since the cylindrical shape of a candle is established as the optimal candle shape, the next step is to explore the distribution of heat from the flame for a cylindrical candle to determine the optimal size for a cylindrical candle. The distribution of heat, U , above the surface of

a cylindrical candle is described by the heat equation in circular polar coordinates.

$$\frac{\partial^2 U}{\partial r^2} + \frac{1}{r} \frac{\partial U}{\partial r} + \frac{1}{r^2} \frac{\partial^2 U}{\partial \theta^2} = \frac{1}{D} \frac{\partial U}{\partial t} \quad (1)$$

Since the wick used is cylindrical and has a circular cross-section, the heat above the candle has no angular dependence. Similarly, it is assumed that the heat distribution remains constant for all time until the entire wax has been used. Applying these two assumptions, the following is obtained.

$$\frac{d^2 U}{dr^2} + \frac{1}{r} \frac{dU}{dr} = 0 \quad (2)$$

Upon solving this ODE, we arrived at a general solution of the form.

$$U(r) = A \log(r) + B \quad (3)$$

where A and B are real constants. Since the heat energy, $U(r)$ is directly proportional to the temperature at r , if we divide Eq.3 by a constant of proportionality (the heat capacity of the wax), we have an equation for the temperature at a distance r from the wick. However, dividing the equation by a constant wouldn't change its structure since A and B are constants. Hence, we can treat $U(r)$ as a temperature. That being said, two conditions need to hold. The first is that the temperature close to the wick, at $r = w$, where w is the wick radius (which is sufficiently close to the centre of the wick) is the wick temperature, T . Secondly, since the temperature decays further away from the wick, there will be a point where the air around the wax won't be hot enough to melt it. If the melting point of the wax is θ_* , then it's required that at $r = R$ for the optimal (or maximal) radius, $U(R) = \theta_*$. Assuming this, we obtained

$$U(r) = \frac{T - \theta_*}{\log(\frac{w}{R})} \log\left(\frac{r}{R}\right) + \theta_* \quad (4)$$

$$\Rightarrow U(r) = \frac{T - \theta_*}{\log(\frac{w}{R})} \log(r) - \frac{T - \theta_*}{\log(\frac{w}{R})} \log(R) + \theta_* \quad (5)$$

as the equation for the heat distribution above the candle surface where $U(r)$, is the temperature of the wax at distance r from the wick and $-\frac{T - \theta_*}{\log(\frac{w}{R})} \log(R) + \theta_*$ is a constant. This equation can be used to experimentally determine the optimal candle radius. If a graph of $U(r)$ against $\log(r)$ is plotted, then the gradient will be the negative constant $\frac{T - \theta_*}{\log(\frac{w}{R})}$ where θ_* , T and w can be measured. The optimal candle radius can be found from the gradient of this graph for the chosen wick to ensure the melting point is reached at the edge of the candle. The value of this gradient should be universal for all optimal candles. Therefore, we will call this constant the 'optimal candle

constant', C . Once we measure this constant, we can begin constructing the optimal candle with the maximum luminosity. We assumed that ratios between lengths and areas are conserved for optimal candles. Hence, using the optimal candle constant, we can say that the temperature for any optimal candle is given by

$$T = C \log\left(\frac{w}{R}\right) + \theta_* \quad (6)$$

where R is the radius of the candle. Using the Stefan-Boltzmann law together with this new definition of wick temperature, we get an equation for the maximum luminosity for any cylindrical candle of radius R .

$$L_{max} = \sigma A_{wick} [C \log\left(\frac{w}{R}\right) + \theta_*]^4 \quad (7)$$

Since we assumed the ratios between areas and lengths are constant for all optimal candles, the ratio between the wick surface area and the candle surface can be said to be a constant (Eq.8). We can find this ratio by using the theoretical optimal candle radius for the wick used to construct the $U(r)/\log(r)$ plot and the surface area of the wick used. Obtaining this constant, an equation for the maximum surface area of the wick can be found which will produce maximum luminosity.

$$A_{wick} = kR^2 \quad (8)$$

$$\Rightarrow L_{max} = \sigma kR^2 [C \log\left(\frac{w}{R}\right) + \theta_*]^4 \quad (9)$$

3 Experimental Evaluation

3.1 Method

3.1.1 Sample Preparation

Beeswax candles of cylindrical and cuboidal shapes were fabricated using different methods. For cylindrical candles, a wick was positioned at one end of a beeswax sheet, which was then rolled around the wick. Cuboidal candles were prepared by folding a beeswax sheet around a centrally placed wick. Due to limited experimental time, only five sample candles were produced. Candles No. 2 and No. 3 (Table 1) were equipped with NT35 wicks to investigate the impact of geometry on burning efficiency and wax consumption. Candles No. 1, No. 4, and No. 5 (Table 1) were fitted with NT23 wicks, with Candles No. 4 and No. 5 used for determining the optimal candle constant (C). Candle No. 1 was employed to assess the warm-up time required for the candle before measurements were initiated and to observe potential tunnelling effects during combustion. Subsequently, the diameters of the wicks were measured using a digital vernier calliper. The radius of each candle was determined at multiple points: both ends, the middle, and a random position between the top and the middle,

with two perpendicular measurements taken at each location, yielding a total of eight measurements. The average of these measurements was used to calculate the overall diameter of the candle. The height of the candle, including the wick, as well as the height of the wax portion, were also recorded using the digital vernier calliper. The exposed wick length was derived by subtracting the wax height from the total height. The initial mass of each candle was measured with a digital mass balance. Following the setup of the experimental apparatus (Figure 2) and ensuring the laboratory environment was adequately darkened, a background illuminance reading was taken using a lux meter. Candle No. 1 was then lit and monitored with a stopwatch to determine the necessary warm-up time for establishing a sufficient wax pool. The warm-up time, derived from the methods described in [1] and [5], was determined to be 30 minutes. The warm-up time for candles refers to the period required for the candle to burn long enough for the wax to form a sufficient melt pool around the wick to achieve stable combustion.^{[1][5]} Then the melting point of the wax was determined by heating 5 of $3\text{cm} \times 3\text{cm}$ beeswax sheets as samples until they just melted, with the temperatures recorded. This process was repeated five times to obtain an average melting point.

3.1.2 Cylinder vs Cuboid

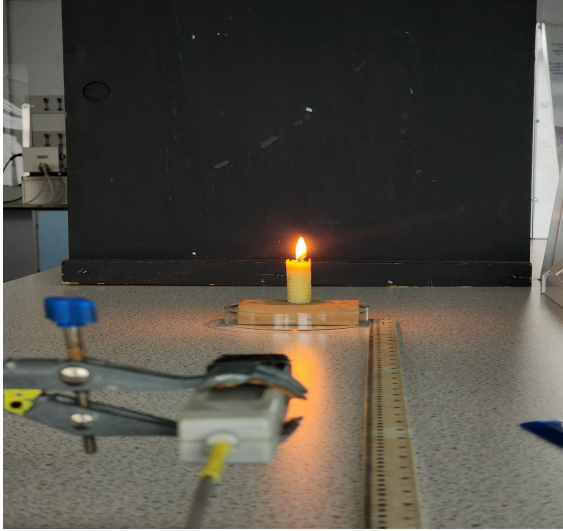


Figure 2: Experimental Setup for measuring illuminance using a Lux meter. In the foreground of the image lux meter probe with its holder can be seen in line with the candle flame

Upon completion of sample preparation and warm-up time determination, Candle No. 2 was ignited and allowed to burn for 30 minutes. The lux meter probe was then positioned closer to the candle, with the height of the probe holder adjusted to align the candle flame with the probe.

3.2 Results

The melting point of the beeswax was calculated as $62.00^\circ \pm 0.04^\circ \text{C}$. Using the gradient obtained from fig.3 that was plotted for candle no.4, the optimal candle constant was calculated as $(-5 \pm 2)\text{K}$. The 'k' of Eq.8 was calculated as 0.33 ± 0.08 .

The distance between the candle flame and the probe was gradually increased until the lux meter displayed a measurable value. This distance was subsequently measured using a set square and a meter ruler. By following this procedure, an optimal distance of $85.50 \text{ cm} \pm 0.01 \text{ cm}$ from the candle to the front of the probe was identified, ensuring accurate illuminance readings while preventing saturation and minimizing the influence of surrounding light, as governed by the inverse square law. This distance was adopted for all subsequent illuminance measurements. After an additional 30 minutes, the second illuminance measurement was taken by adjusting the probe height according to the same procedure and positioning the probe at the previously established location. A third illuminance measurement was performed 30 minutes after the second, following the same method. During the intervals between illuminance measurements, thermal images of the candle were captured using a Hikmicro B20 thermal imaging camera, positioned horizontally to the candle, to observe the radial heat distribution of the candle flame [6]. The same procedure applied to Candle No. 2 was repeated for Candle No. 3. Once both Candles No. 2 and No. 3 had completely burned, their final masses were recorded using a digital scale. At last, the fuel efficiency was determined based on the initial and final masses of the candles.

3.1.3 Determining the optimal candle constant

A similar procedure was followed for Candle No. 4 to obtain illuminance measurements. However, after the third measurement, the candle flame was extinguished. The temperature at and around the wick was then assessed using a Hikmicro B20 thermal imaging camera [6]. The camera was positioned above the candle to capture a cross-sectional image of the flame. It is important to note that the camera was slightly angled to avoid direct alignment with the flame, thus preventing potential damage to the lens. Next, Candle No. 5 (Table 1) was ignited; however, illuminance measurements were not conducted due to the rapid combustion of the candle and the instability of the flickering flame. The candle was allowed to burn out without further measurements. Subsequently, a graph was constructed plotting the temperature of the wax against the natural logarithm of the distance from the centre of the wick for Candle No. 4. The gradient of this graph was obtained using the Microsoft Excel LINEST function. The parameter 'k' was then calculated using Equation 8. Using the calculated optimal candle constant, the temperature at the wick was determined for the maximum radius (25 mm) of a single-wicked candle, as recommended by the manufacturer [7]. Finally, the maximum luminosity for the optimal candle with a radius of 25 mm was calculated.

Then the New temperature at the wick (NT23) for the optimal candle radius 25mm was calculated as $(352 \pm 6)K$ and luminosity was calculated as $(0.18 \pm 0.01)W$.

Candle No.	Candle Shape	Initial Mass(g) $\pm 0.01g$	Diameter(mm) $\pm 0.004mm$	Height(mm) $\pm 0.007mm$
1	Cylindrical	17.37	41.967	23.450
2	Cylindrical	13.43	22.936	65.840
3	Cuboidal	16.50	width 11.20/ length 83.26	32.250
4	Cylindrical	33.59	35.726	66.080
5	Cylindrical	10.73	19.460	68.810

Table 1: Properties of the beeswax sample candles

Candle No.	Exposed wick length(mm) $\pm 0.01mm$	Wick Diameter(mm) $\pm 0.01mm$	Wick Type
1	15.00	2.42	NT23
2	16.93	3.64	NT35
3	14.05	3.64	NT35
4	13.31	2.42	NT23
5	11.39	2.42	NT23

Table 2: Dimensions of the wick utilized in each candle

Candle No.	Candle Shape	Initial Wax Mass(g) $\pm 0.01g$	Final Wax Mass (g) $\pm 0.01g$	Fuel Efficiency (%)
2	Cylindrical	13.43	1.39	89.65
3	Cuboidal	16.50	10.30	37.57

Table 3: Comparison of fuel efficiency for cylindrical and cuboidal candles.

Candle No.	Measurement I $\pm 5Lux$	Measurement II $\pm 5Lux$	Measurement III $\pm 5Lux$
2	173	165	170
3	170	160	180
4	180	183	181

Table 4: Illuminance measurement of the candles after deducting the background reading, measured as $(22.0 \pm 0.7)Lux$ using a Lux meter

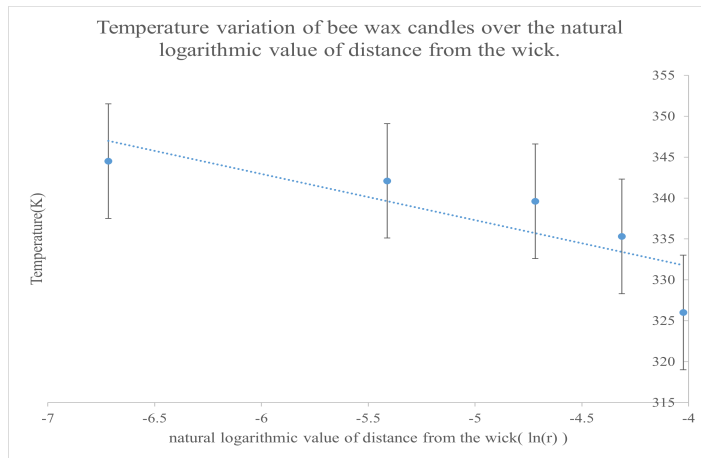


Figure 3: Temperature variation of beeswax candles with NT23 wicks over the natural logarithmic value of the distance from the centre of the wick.

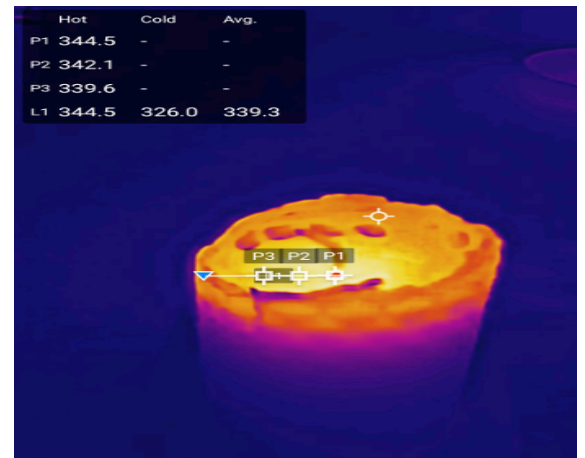


Figure 4: Thermal image of the cylindrical candle (Candle No.4).

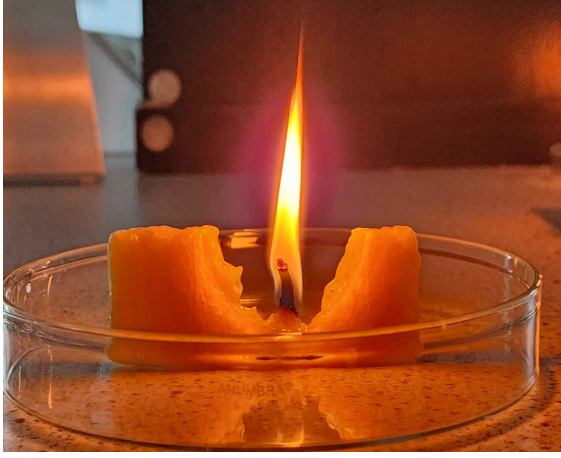


Figure 5: Cuboidal candle (Candle No.3) showing unmelted wax on the far sides and tunnelling.



Figure 6: Thermal Image of the cuboidal shape candle(Candle No.3)

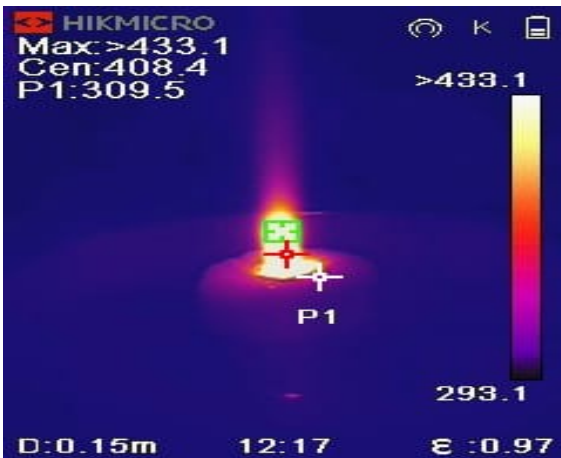


Figure 7: Thermal image of a cylindrical candle (Candle No.2) with (22.97 ± 0.02) diameter

4 Discussion

The selection of cylindrical and cuboidal shapes for the candle designs was guided by the requirement for a constant cross-sectional area, a critical condition for maintaining a consistent wax pool size and, consequently, constant

luminosity. This criterion can be achieved with geometries such as cylinders, cubes, and cuboids. The results presented in Table 4 demonstrate that cylindrical candles maintained constant illuminance within the error margins of the measurements. A cuboidal shape was chosen over a cubic shape for comparison against the cylinder to highlight that a larger cross-sectional area does not inherently guarantee maximum luminosity but rather ensures constant luminosity, as outlined in the theoretical model. This is further substantiated by the experimental results for Candles No. 2 and 3 in Table 4. The observed differences are attributed to the radial heat distribution evident in the thermal images (Figure 67). The behaviour of Candle No. 5, which exhibited incomplete combustion, leading to soot accumulation and a flickering flame, underscores the importance of combustion stability in achieving consistent performance. Analysis of the fuel efficiency values in Table 3 supports the theoretical predictions regarding the impact of geometry on wax melting patterns and fuel efficiency. Observations from the cuboidal candle experiment revealed efficient wax melting near the wick, while the outer regions remained largely unmelted (Figure 5). This outcome underscores the significance of radial heat distribution, as the symmetrical geometry of cylindrical candles facilitates even heat dispersion, ensuring uniform wax melting. In contrast, the asymmetrical shape of cuboidal candles leads to uneven heat distribution, resulting in tunnelling effects (Figure 5), where wax depletion occurs near the wick while large portions of the candle remain unused. Quantitatively, cylindrical candles demonstrated superior fuel efficiency, utilizing $89.65\% \pm 0.01\%$ of the wax mass during complete combustion, compared to the cuboidal candle, which achieved only 37.57% fuel efficiency due to unmelted wax at the edges and corners. These findings highlight the advantages of cylindrical geometry in aligning with the natural radial heat distribution of the flame, ensuring consistent wax melting and optimal fuel utilization. Theoretical predictions were validated with a negative value for the optimal candle constant and a calculated wick temperature for the maximum recommended radius (25 mm) of a single-wicked candle, as specified by the manufacturer [7]. However, the calculated luminosity was lower than anticipated, likely due to inaccuracies in measuring the wick temperature and corresponding distances immediately after flame extinguishment rather than during combustion. Efforts to measure flame temperature using a digital K-type thermocouple revealed a flame temperature of 1010°C . The limited number of measurements was due to soot build-up on the thermocouple, which affected data accuracy. Additionally, the cylindrical candle (Candle No. 2) with a diameter of $(22.97 \pm 0.02)\text{mm}$ generated $173 \text{ Lux} \pm 5 \text{ Lux}$, exceeding the illuminance of the cuboidal candle (Candle No. 3), which produced $170 \text{ Lux} \pm 5 \text{ Lux}$. Furthermore, as the candle diameter increased, illuminance also increased, with Candle No. 4 (diameter $(35.73 \pm 0.02)\text{mm}$) producing $180 \text{ Lux} \pm 5 \text{ Lux}$ (Table 4). Future work could include a modified theoretical model incorporating the relationship between the wick temperature before and after flame extinguishment through an additional constant, enhancing

the accuracy of predictions.

5 Conclusion

Through a combination of theoretical modelling and experimental evaluation, it was confirmed that cylindrical candles are the most efficient geometry for achieving optimal fuel utilization. This efficiency was demonstrated by the minimal mass of wax remaining after the wick was fully burned out. Additionally, it was observed that the luminosity of the candle increased with an increase in its radius. However, this increase is constrained by practical limitations, such as tunnelling effects and wick mushrooming, which are influenced by the wick's diameter and material properties. For future improvements in experimental evaluation, it is recommended to measure the temperature of the wax in real time while the wick is burning. Such measurements would provide more accurate data for refining the theoretical model and enhancing the understanding of the relationship between candle geometry, heat distribution, and overall performance.

References

- [1] A. N. Furlong, J. B. Haelssig, and M. J. Pegg, "Impact of candle wicks and fuels on burning rate, flame shape, and melt pool diameter," *Journal of Candle Science*, vol. 10, no. 2, pp. 123–135, 2023. [Online]. Available: https://www.researchgate.net/publication/367298005_Impact_of_candle_wicks_and_fuels_on_burning_rate_flame_shape_and_melt_pool_diameter
- [2] M. Faraday and F. A. J. L. James, *The Chemical History of a Candle*, 1st ed. Oxford, England: Oxford University Press, 2011.
- [3] Harlem Candle Company, "Candle care 101: How to fix & prevent candle tunneling," 2025, accessed: 2025-01-07. [Online]. Available: https://www.harlembrands.com/blogs/journal/candle-care-101-how-to-fix-prevent-candle-tunneling?utm_source=chatgpt.com
- [4] A. Hamins, M. Bundy, and J. C. Yang, "Characterization of candle flames," *Combustion and Flame*, vol. 157, no. 9, pp. 1634–1639, 2010. [Online]. Available: <https://www.sciencedirect.com/science/article/pii/S1540748910001665?via%3Dihub>
- [5] CandleScience, "How to conduct a burn test," 2025, accessed: 2025-01-07. [Online]. Available: https://www.candlescience.com/learning/how-to-conduct-a-burn-test/?srsltid=AfmBOorF95XbvLUbDDTOodBUPN47LUfrbUZjVXdyY_buJo96slMJpDcx&utm_source=chatgpt.com
- [6] HIKMICRO, *Thermal Imaging Camera User Manual*, 2021, accessed: 2025-01-07. [Online]. Available: <https://webassets.hikmicrotech.com/global/asset/50586362eddb480d9c8b48e7a03fb3b8.pdf>
- [7] 4Candles, "Raw unwaxed candle wicks," accessed: 2025-01-06. [Online]. Available: <https://www.4candles.co.uk/candle-making-wick/raw-unwaxed.html>